Simulation of Microwave Integrated Circuit on Multilayered Resistive Substrats using Wave Concept Iterative Procedure

Somsak Akatimagool

Department of teacher training in electrical engineering, Faculty of technical education,
King Mongut's Institute of Technology North Bangkok
1518, Pibulsongkram Road, Bangsue, Bangkok 10800, Thailand
Tel: (+66)0-2913-2500 ext. 3242 Fax: (+66) 0-2587-8255
e-mail: ssa@kmitnb.ac.th

Abstract : This paper presents the iterative procedure with the concept of expanded waves in the spectral and spatial domains using the fast modal algorithm. We presents its applications to microwave integrated circuits on resistive substrate. The advantage is a reduction in computation time. These calculated results are checked by comparison with the experimental and simulated results by Sonnet and Momentum program.

Keywords : wave, iterative, electromagnetic, simulation, microwave integrated circuit

1. Introduction

Microwave circuits are characterised by one or several thin metallic layers containing passive and active elements. Between these layers, the dielectric medium is most often homogeneous.

The more methods for the simulation of microwave integrated circuits are base on an integral formulation solved with a method of moments. This method requires a set of two dimension basis functions chosen in the plan of circuit. Another method concerns the Transmission Line Matrix (*TLM*) method. It combines the advantages of the iterative scheme and the easy representation of the homogeneous spaces in the spectral domain. The spectral domain is preferred rather than the time domain because of the very complicated response of a half free space in the time domain.

The general principle in this paper, concerns the iterative methods of the conception of the waves with fast modal algorithm "Wave Concept Iterative Procedure (*WCIP*) "[1-5] . This method presents the alternating between the spatial domain (pixel) and the spectral domain (modes). In the electromagnetic scattering, on the surface of the circuit, the boundary conditions are presented in several sub-domains; the metal, the insulating and the source. For a speed of the resolution, we benefit the Fast Fourier Transform (*FFT*) expression.

In this work, We will focus on spiral inductors and patch antenna with the Wave Concept Iterative Procedure. The spatial domain provides the versatility in circuit description while spectral domain ensures reliable description of multi-layer substrates.

2. Method of Analysis

The boundary conditions on the planar circuit are also defined in term of waves. The balance condition between boundary and external conditions provides the iterative procedure. On the printed surfaces see the fig.1, the boundary conditions are expressed in term of waves rather than in terms of tangential fields. According to the surface, incident and reflected waves (*A* and *B*) are defined as :

$$A = \frac{1}{2\sqrt{Z_0}}\left(E_t + Z_0 H_t \wedge n\right) \qquad (1)$$

$$B = \frac{1}{2\sqrt{Z_0}}\left(E_t - Z_0 H_t \wedge n\right) \qquad (2)$$

when Z_0 is an arbitrary wave impedance, E_t and H_t are the electric and magnetic tangential fields to the surface and n the outgoint normal to the surface.

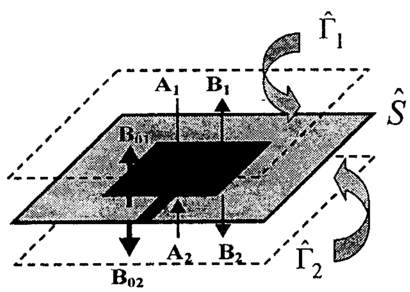

Fig. 1 printed surface of circuit and incident and reflected waves

As a result, the set of boundary conditions defines an integral diffraction operator $\hat{S}$ built in the spatial domain. The numerical representation of $\hat{S}$ is achieved with a basis of pixel-like functions. Then, the iterative procedure rests on the balance conditions between the diffracted waves by the printed surfaces and the reflected waves by the circuit environment : substrate and enclosure.

The boundary conditions on tangential fields are translated in terms of waves see in the fig.1; on the metallic sub-domain : D_M, the cancellation condition of tangential electric fields $E_1 = E_2 = 0$ (the subscript

$i=1,2$ refers to the two sides of the printed surface) yields, from the definition (1)-(2), the following S matrix to represent the continuity conditions :

$$\begin{bmatrix} B_1 \\ B_2 \end{bmatrix}_M = \begin{bmatrix} -1 & 0 \\ 0 & -1 \end{bmatrix} \begin{bmatrix} A_1 \\ A_2 \end{bmatrix}_M \qquad (3)$$

On the dielectric sub-domain : D_D, the conditions $E_1 = E_2$ and $J_1 + J_2 = 0$ give :

$$\begin{bmatrix} B_1 \\ B_2 \end{bmatrix}_D = \begin{bmatrix} \frac{1-n^2}{n^2+1} & \frac{2n}{n^2+1} \\ \frac{2n}{n^2+1} & \frac{n^2-1}{n^2+1} \end{bmatrix} \begin{bmatrix} A_1 \\ A_2 \end{bmatrix}_D \qquad (4)$$

while, on the source sub-domain : D_S, $E_1 = E_0 - Z_0(J_1 + J_2)$ give :

$$\begin{bmatrix} B_1 \\ B_2 \end{bmatrix}_S = \begin{bmatrix} \frac{-1+n_1-n_2}{1+n_1+n_2} & \frac{2n_{12}}{1+n_1+n_2} \\ \frac{2n_{12}}{1+n_1+n_2} & \frac{-1-n_1+n_2}{1+n_1+n_2} \end{bmatrix} \begin{bmatrix} A_1 \\ A_2 \end{bmatrix}_S \qquad (5)$$

where $n = \sqrt{\frac{Z_1}{Z_2}}$, $n_{12} = \frac{Z_0}{\sqrt{Z_1 Z_2}}$, $n_1 = \frac{Z_0}{Z_1}$ and $n_2 = \frac{Z_0}{Z_2}$.

The advantage of this 2.5D environment is preserved by using a reflection operator defined in the spectral domain from the admittance operator as :

$$\hat{\Gamma} = \sum_n |f_n\rangle \Gamma_n \langle f_n| \quad with \quad \Gamma_n = \frac{1 - Z_0 Y_{mn}}{1 + Z_0 Y_{mn}} \qquad (6)$$

when Y_{mn} are the eigen values of the admittance operator. Substrate resistivity and layer stacking are included in these eigen values. The toggling between the spectral and spatial domains is insured by a fast modal transform based on a fast fourier transform.

3. Iterative Procedure

The printed surface being discretized by pixel-like functions, collecting for each sub-domain the S-relations (3)-(5) described in the previous section, the scheme of the successive iterations is given by :

$$\begin{aligned} B &= \hat{S} A + B_0 \quad \textit{in the spatial domain} \\ A &= \hat{\Gamma} B \quad \textit{in the spectral domain} \end{aligned} \qquad (7)$$

The toggling between the spatial and the spectral representation of the waves A and B is ensured by a fast modal transform quite similar to the Fast Fourier Transform (*FFT*) which takes advantages in the pixel-like discretization of the printed surface of the circuit.

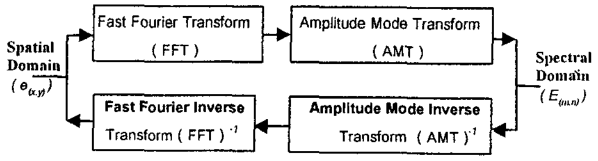

(II)

Fig.2 Diagram of fast modal algorithm

The formulation spectral of the wave is base on the box with electric mural define in term of the electric field as :

$$\vec{E}^{\alpha}_{x(x,y)} = K^{\alpha}_x \cos\left(\frac{m\pi x}{a}\right) \sin\left(\frac{n\pi y}{b}\right) \qquad (8)$$

$$\vec{E}^{\alpha}_{y(x,y)} = K^{\alpha}_y \sin\left(\frac{m\pi x}{a}\right) \cos\left(\frac{n\pi y}{b}\right) \qquad (9)$$

with α refer to the *TE* and *TM* mode , a and b refer to the dimension of the box and K refer to the value constant with respect to the x and y direction.

The definition is base on the Fast Modal algorithm (*FFT_mod*) extended to include two parts see in the fig.2, a Fast Fourier Transform and a Mode Transform. If M and N are mapped into the matrix of the two dimensions, a cosine and sine Discrete Fourier transform (*DFT*) of $M \times N$ pixels is a separable transform in the x-polarisation defined as [10-11]:

$$E^{\alpha}_{x(m,n)} = \beta_{(m)} \gamma_{(n)} \sum_{x=0}^{M-1} \sum_{y=0}^{N-1} E^{\alpha}_{x(x,y)} \cos\left(\frac{\pi(2x+1)m}{2M}\right) \sin\left(\frac{\pi(y+1)(n+1)}{N+1}\right)$$

$$with \begin{cases} for & 0 \le m \le M-1 \\ for & 0 \le n \le N-1 \end{cases} \qquad (10)$$

while a cosine and sine inverse Discrete Fourier transform $(DFT)^{-1}$ of $M \times N$ pixels in the x-polarisation defined as (11) :

$$e^{\alpha}_{x(x,y)} = \sum_{m=0}^{M-1} \sum_{n=0}^{N-1} \beta_{(m)} \gamma_{(n)} E^{\alpha}_{x(m,n)} \cos\left(\frac{\pi(2x+1)m}{2M}\right) \sin\left(\frac{\pi(y+1)(n+1)}{N+1}\right)$$

$$with \begin{cases} for & 0 \le x \le M-1 \\ for & 0 \le y \le N-1 \end{cases} \qquad (11)$$

while $\beta_{(0)} = \sqrt{\frac{1}{M}}$, $\beta_{(m)} = \sqrt{\frac{2}{M}}$ for $1 \le m \le M-1$ and,

$\gamma_{(n)} = \sqrt{\frac{2}{N+1}}$ for $0 \le n \le N-1$.

However, in the same way we can also obtain the *DFT* and the inverse *DFT* for the y-polarisation. The *DFT* algorithm can implement a fast algorithm. The *FFT* algorithms require $P=2^n$ where n is a positive integer.

4. Numerical Results

In this section, we present some examples to illustrate the application of WCIP simulation.

4.1 Time computation of simulation

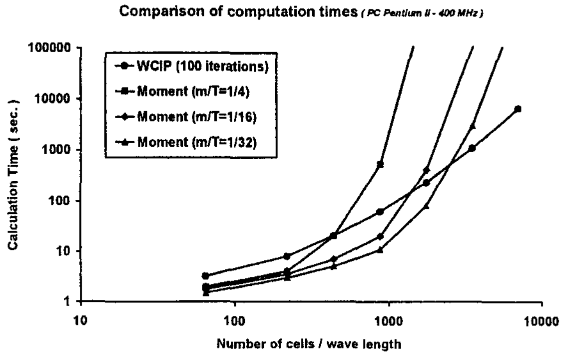

Fig. 3 Comparison between Moment method and WCIP computation times versus the pixel size for different m/T ratio

Figure 3 compares the computation time versus the pixels size between WCIP and moment method for three values of the ratio (*m/T*) between the metal surface and the total surface. As the pixel size is arround one thousandth of wave length, the saving of computation time is about one decade with *WCIP* for a *m/T*=0.25 ratio which is not favourable to *WCIP*.

4.2 Spiral inductors

The four turns of spiral inductor in fig.4 is now studied [5-8]. The conductors (w) are 8.67, 13 and 17.34 µm wide and the line spacing (s) are 17.34, 13 and 8.67 µm wide, the overall dimensions is fixed of 226 µm² and the calculated parameters of spiral inductor displayed in table 1.

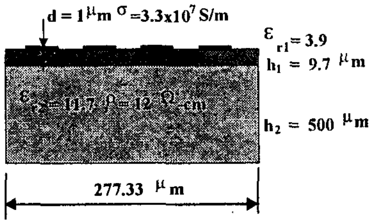

(a)

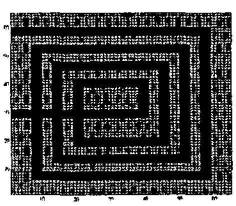

(b)

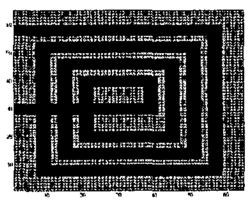

(c)

Fig. 4 (a) IC's structure (b) Spiral inductor (w/s = 1) and (c) Spiral inductor (w/s = 2)

Table 1 Comparaison of results between the WCIP Simulation and SONNET (w/s = 0.5, 1 and 2 respectively)

(w/s)	Calculus	Ls nH	Rs Ω	Cp fF	Rp Ω	Q max	f_{max} GHz
0.5	Sonnet	2.26	8.7	64	1000	4.4	4.5
	WCIP	2.24	6.7	79	750	4.5	4.5
1	Sonnet	2.00	5.7	71	825	5.7	4.5
	WCIP	2.06	5.1	74	930	5.2	4.5
2	Sonnet	1.71	4.8	75	735	5.8	4.5
	WCIP	1.76	3.7	73	850	6.6	4.5

Table 1 presents the comparison of inductors parameters between the WCIP and Sonnet Simulation. These results of the spiral inductor are extracted from the calculated scattering matrix or/ admittance matrix of the lumped elements in the π-network of the spiral inductance is deduced by the expression given by Yue and Wong [5].

4.3 Patch antenna

The coupling of two patch antennas is now studied in fig.5. The resonance frequency of one patch is 4.95 GHz. This calculating is checked by comparison in the fig.6 with the experimental results.

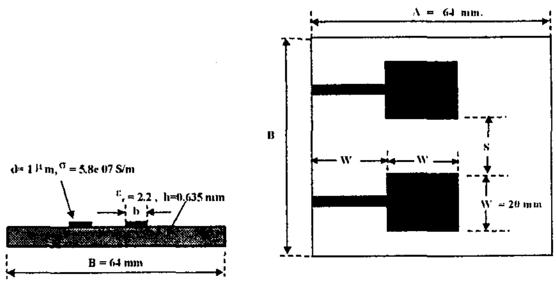

(a) *(b)*

Fig. 5 (a) IC's structure and (b) Patch antenna

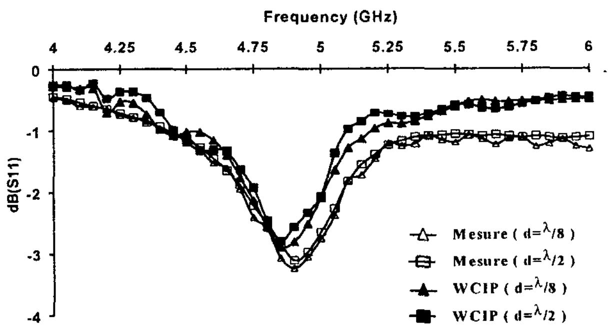

Fig. 6 Comparison of parameter S_{11} in decibel between the WCIP and experimental results

Morever, using of this *WCIP* method, the current distribution and the electric field of the three dimension can be obtained (see in the fig.7). The magnitude of the electric field distributes on the dielectric medium of the circuit and the magnitude of current density exists on the conductor of the patch antennas.

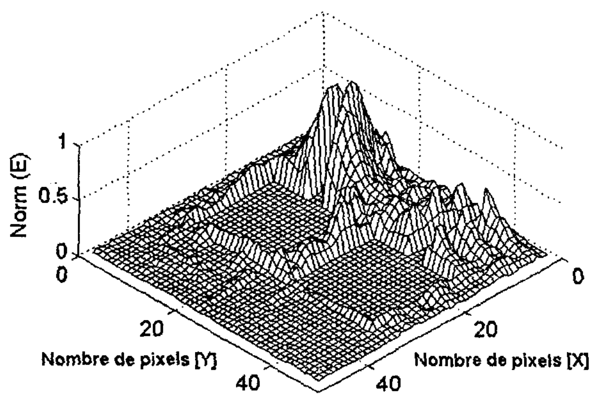

(a)

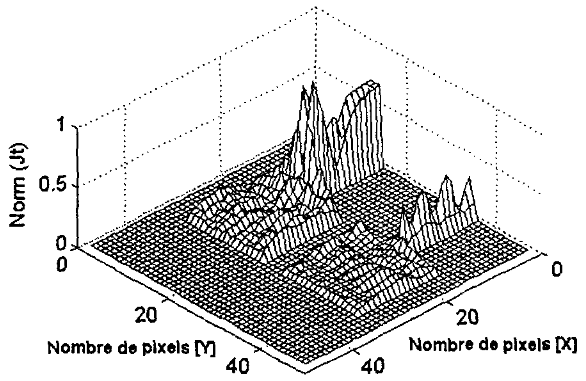

(b)

Fig. 4 (a) Electric field and (b) Current density distribution

5. Conclusion

The WCIP simulation is a new method for the 2D electromagnetic simulation. We have presented the complex description of electric and magnetic field and applied it to the simulation of microwave integrated circuits. The simulation data for all of the examples in this paper have been found to be in good agreement with the experimental and other simulation results. This method appears as an efficient alternative to the standard moment method in these 2.5D configurations.

6. Acknowledgement

The author would like to thank Prof. Bajon, Ecole Natioanle Superieur de l'Aeronautique et de l'Espace and Prof. Baudrand, Ecole Nationale Superieur d'Electro-technique d'Electronique d'Informatique d'Hydraulique de Toulouse, France for helpful discussions and for providing the experimental data.

References

[1] S.Akatimagool, D.Bajon, H.Baudrand, "Analysis of Multi-layer Integrated Inductor with Wave Concept Iterative Procesdure (WCIP)", *IEEE MTT-S Intern. Microwave Symp. Digest.*, Arizona, USA., May 2001.

[2] S.Akatimagool, D.Bajon, H.Baudrand, "Modelisation of Microwave Interconnects IC's with Iterative Procedure using Fast Modal Algorithm", *Progress in Electromagnetics Research Symp. (PIRES),* Osaka, Japan, July 2001.

[3] H.Baudrand "The Wave Concept in Electro-magnetic Problems : Application in Integral Methods", *Asia Pacific Microwave Conference APMC'96,* New Dehli, 1996.

[4] F.Bouzidi, H.Aubert, D.Bajon, H.Baudrand, "Equivalent network representation of boundary conditions involving generalized trial quantities: Application to lossy transmission lines with finite metallization thickness ". *IEEE Trans. on Microwave Theory and Techniques*, Vol. 45, N° 6, pp. 869–876, June 1997.

[5] C.Patrick Yue, S.Simon Wong; "On-Chip Spiral Inductors with Patterned Ground Shields for Si-Based RF IC's", *IEEE Journal of Solid-State Circuit*, Vol 33, No. 5, may 1998.

[6] J.N.Burghartz, Keith A.Jenkins; "Multilevel-Spiral Inductors Using VLSI Interconnect Technology", *IEEE Electron Device Letters,* Vol. 17, No.9, September 1996.

[7] A. M. Niknejad, Robert G.Meyer, Fellow,"Analysis, Design and Optimization of Spiral Inductor and Transformers for Si RF IC's", *IEEE journal of solid-state circuit,* vol. 33, No. 10, October 1998.

[8] T.Becks, I.Wolff; "Analysis of 3-D Metallization Structures by a Full-Wave Spectral Domain Technology", *IEEE Transactions on Microwave Theory and Techniques*, Vol.40, No.12, December 1992.

[9] Anil K., "*Fundamental of Digital Image Processing*" , Prentice- Hall, Englewood Cliffs, NJ, 1989.

[10] Ronald N. Bracewell, "*The Fourier Transform and Its Applications*", McGraw Hill, Third edition, 2001.